Moving Photovoltaic (PV) Installations: Impacts of the Solar Radiation Level on the Output Power

Christian Schuss*, Tapio Fabritius†, Bernd Eichberger‡, and Timo Rahkonen*
*Circuits and Systems (CAS) Research Unit, University of Oulu, Finland; email: christian.schuss, timo.rahkonen@oulu.fi
†Optoelectronics and Measurement Techniques Research Unit, University of Oulu, Finland; email: tapio.fabritius@oulu.fi
‡Institute of Electronic Sensor Systems, Graz University of Technology, Austria; email: bernd.eichberger@tugraz.at

***Abstract*—This paper investigates the potential output power of moving photovoltaic (PV) installations. In particular, we focus on the impacts of the solar radiation level on the available output power of PV installations on top of moving objects. We discuss the situation for controlling the operating voltage of photovoltaics installed on top of battery-powered electric vehicles (BEVs) and hybrid electric vehicles (HEVs). We demonstrate that different longitudinal angles of PV cells due to curved roof surfaces and the fast slopes of the solar radiation level have a significant impact on the maximum power point tracking (MPPT) algorithm. We illustrate how the solar radiation level can reduce the efficiency of the MPPT algorithms.**

***Index Terms*—battery-powered electric vehicle, data acquisition, hybrid electric vehicle, measurement, photovoltaic energy.**

I. Introduction

Solar energy is recognized as one of the most promising energy sources of the future [1], in particular to substitute energy gained from fossil fuels such as oil, coal and gas [2]. By integrating photovoltaic (PV) cells into the roof of battery-powered vehicles (BEVs) and hybrid electric vehicles (HEVs), the electrical driving range of these types of vehicles can be extended remarkably [3]–[6]. Similarly, photovoltaics can be used to power a charging station for BEVs and HEVs, for example [7]. However, installing PV cells on top of BEVs and HEVs offers the opportunity to provide electricity to the on-board power supply during driving conditions [3]–[6].

Over the past decades, the electricity consumption of automobiles has grown significantly due to the increased deployment of electronic control units (ECUs) [8]. Their objectives include the control of the power train, as well as safety and comfort requirements. In the case of HEVs, an additional demand of 100 Watts electrical power increases the fuel consumption by 0.1 to 0.2 litres per 100 kilometres [8], [9]. Similarly, in the case of BEVs, the electrical driving distance is reduced by electronics.

Photovoltaics do not provide sufficient power for the propulsion of BEVs and HEVs [10]. Hence, we suggest to use PV energy as an energy range extender (ERE). For BEVS, PV energy can be supplied to non-critical systems within the on-board power grid when driving. In the case of HEVs, the amount of electricity which has to be provided by the alternator can be reduced. For both types of vehicles, the high-voltage battery can be charged by the PV installation when the vehicle is parked.

Unfortunately, the available area for PV cells on top of BEVs and HEVs is limited. In addition, due to the curved shape of the roof, PV cells are oriented under different longitudinal angles towards the sun. These circumstances have an impact on the available output power of the PV installation [3]–[6]. Fig. 1 shows the experimental vehicle, a Toyota Prius, which was used for analysing the impact of different orientations of PV cells towards the sun. Fig. 2 illustrates the available area for PV cells on the roof of the Toyota Prius.

Fig. 1. Experimental vehicle with integrated PV cells on the roof

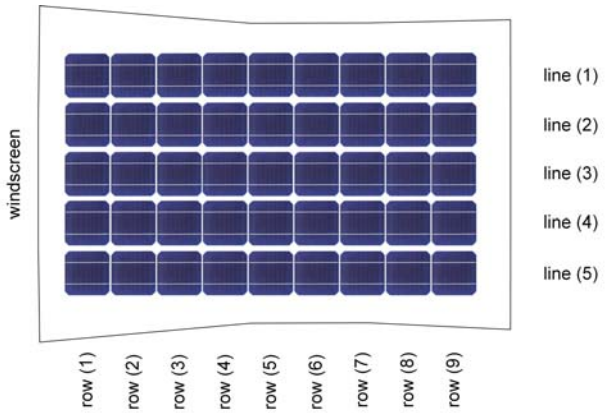

Fig. 2. PV installation on top of the experimental vehicle

In this paper, we extend our analysis from [11] in two ways. Firstly, we investigate the impact of the solar radiation level (λ) on the available output power (P_{out}) of each PV cell in the different rows. Secondly, we analyse how the different amount of solar radiation of each PV cell influences the performance of MPPT algorithms, more precisely, the choice of the value of the parameter of the MPPT algorithm. Here, we demonstrate that it is challenging to select a uniform value for the parameter of the algorithm.

II. Experimental Setup

A. Photovoltaics within Experiments

As mentioned above, the available space on top of BEVs and HEVs is limited. Hence, we suggest using superior PV cells with high efficiencies and high output currents. As a result, a significant amount of PV energy can be produced and provided to the on-board power supply of vehicles. In the experiments and, thus, also for the PV simulation model, a monocrystalline silicon (mono-Si) PV cell was used. The dimension of one PV cell is 156 x 156 millimetres. Table I summarises the most important output parameters obtained from the datasheet of the manufacturer Blue Chip Energy GmbH [12].

TABLE I
Data of the Blue Chip PV cell

Parameter	Value
P_{mpp}	4.140 W
V_{mpp}	0.515 V
I_{mpp}	8.039 A
V_{oc}	0.613 V
I_{sc}	8.602 A

AM1.5; λ = 1,000 W/m^2; T_c = 25 °C; standard test conditions (STC)

B. Possible Amount of PV Cells

Due to the curved shape of the roof of the Toyota Prius, it is not possible to utilise 100% of the roof's area for the installation of PV cells [4]. On average, the available area on the roof of BEVs and HEVs varies between 1.5 and 2 m^2. As seen in Fig. 2, the roof of the Toyota Prius is wider at the front than at the back, while it is even smaller in the middle. Hence, for the experimental vehicle, we have chosen a number of 45 PV cells ($n_{\text{cells,row}}$ = 9, $n_{\text{cells,line}}$ = 5), as illustrated in Fig. 2. PV cells are connected in series or parallel in order to increase the output power.

C. The Rate of Change of the Solar Radiation Level

We focus on the rate of change of the solar radiation level (r_λ). In particular, we are interested in the speed of the slope of the solar radiation level (λ), in other words how rapidly the available amount of irradiation is changing. In previous research, we identified the time window to be in seconds for stationary PV installations and in milliseconds for moving PV installations [11]. It is worth noting that r_λ is critical for the choice of the operating voltage of PV cells, and obtained as follows

$$r_\lambda = \frac{\Delta\lambda}{\Delta t} \tag{1}$$

For the case of stationary PV installations, on a typical partly cloudy-sunny day, r_λ can be as large as 150 $\frac{W}{m^2}/s$. Rapid changing ambient conditions can be challenging for some MPPT algorithms, for example for the perturb and observe (P&O) algorithm, the voltage-based MPPT (VMPPT) and current-based MPPT (CMPPT) algorithm [13]. Hence, it is important to analyse the rate of change of the solar radiation level in order to identify possible ways to improve and optimise the performance and efficiency of MPPT algorithms.

III. Output Behaviour of Photovoltaics

A. The Characteristic I-V (Current-Voltage) of a PV cell

Fig. 3 illustrates the characteristic non-linear output behaviour of a PV cell from the manufacturer Blue Chip Energy GmbH in the form of the *I-V* (Current-Voltage) curve and *P-V* (Power-Voltage) curve. The point on the I-V curve, in which the product of voltage and current, the power, becomes a maximum is referred to as the maximum power point (MPP). The available power in the MPP (P_{mpp}) varies with changing ambient conditions such as the solar radiation level (λ) and the PV cell temperature (T_c) [13].

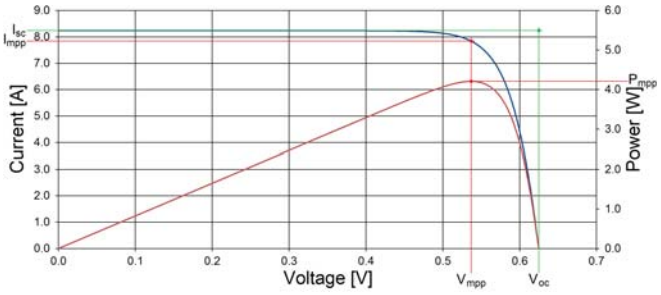

Fig. 3. I-V curve and P-V curve of a PV cell with parameters

B. The VMPPT and CMPPT algorithm

The slope of the solar radiation level and the different longitudinal angles of the PV cells on top of the Toyota Prius have an impact on the performance of MPPT techniques. Basically, MPPT is required to ensure operating at or close to the MPP and, thereby, obtaining as much power as possible from photovoltaics. Esram *et al.* summarised various approaches for carrying out MPPT and investigated differences between MPPT techniques [13]. One of them is the VMPPT algorithm, which is used as an example for MPPT techniques in this work.

In the VMPPT algorithm, for setting the operating voltage (V_{op}), the voltage in the MPP (V_{mpp}) is estimated to be a fraction (M_v) of the open-circuit voltage (V_{oc}), as calculated in Equation (2). As a result, operation does not take place exactly at the MPP, but close to the MPP. One of the benefits of the VMPPT algorithm is the simple implementation. For example, the VMPPT algorithm requires only on sensor to obtain the information on the open-circuit voltage. V_{oc} is

sampled periodically in order to obtain information on the current ambient conditions. Then, V_{op} of the PV cell or panel is alternated accordingly. The value of the factor M_v depends on the material and characteristics of the used PV cell or panel. Values for M_V depend on the PV characteristics, material, encapsulation and configuration [13].

Similarly, in the CMPPT algorithm, the current in the MPP (I_{mmp}) is assumed to be a fraction M_I of the short-circuit current (I_{sc}), as obtained in Equation (3). Here, I_{sc} is measured periodically. In contrast to the VMPPT algorithm, the CMPPT algorithm measures the current instead of the voltage. Hence, the technique is more difficult to implement in practice as it is difficult to measure I_{sc} during operation. Again, values for M_I depend on the PV characteristics, material, encapsulation and configuration [13].

$$V_{mpp} \approx M_V \times V_{oc} \tag{2}$$

$$I_{mpp} \approx M_I \times I_{sc} \tag{3}$$

C. The Perturb and Observe (P&O) algorithm

The P&O algorithm is the most commonly used MPPT technique. Here, the operating voltage (V_{op}) is alternated based on the outcomes of the previous alternation. V_{op} is either increased or decreased, depending on whether the current output power increased or decreased in comparison to the previous measured output power. In contrast to the VMPPT and CMPPT algorithm, both, the voltage and current need to be measured. Moreover, the P&O algorithm does not use an approximation for the position of the MPP, with the continuous measurements of the power of the PV cell, the algorithm tries to find the exact location of the MPP [13].

IV. Available Output Power of PV Installations

A. Orientation of PV cells on top of BEVs and HEVs

Due to the curved shape of the roof of the Toyota Prius, as shown in Fig. 2, PV cells in each row are oriented under a different longitudinal angle (β) towards the sun. As a result, each row of PV cells obtains a different solar radiation level (λ). Table II summarises the different longitudinal angles of the PV cells from row number (1) to (9) on top of the Toyota Prius. As a reference, the street represents the horizontal plane. As seen in Table II, a difference of 24 ° is obtained by comparing the longitudinal angle of PV cells in row number (1) with row number (9).

B. Orientation of the Experimental Vehicle towards the Sun

Under constant irradiation, in other words when the vehicle is in parked conditions, as mentioned above, each row of PV cells receives a different solar radiation level (λ). In the experiments, the front of the vehicle was oriented towards the sun. In this way, PV cells in row number (1) at β = 15 ° were facing the sun, while PV cells in row number (9) at β = – 9 °, for example, were facing away from the sun. This setup was used to measure the open-circuit voltage (V_{oc}) and short-circuit current (I_{sc}) of PV cells, relevant for MPPT algorithms.

C. Impacts on the Open-Circuit Voltage (V_{oc})

Table III presents the obtained values for the open-circuit voltages (V_{oc}) at slightly different solar radiation levels (λ = 570 W/m^2 to 660 W/m^2). λ was measured in row number (6) at β = 0 °. The data was collected under outdoor environmental conditions in the City of Oulu, Finland. For the experiments, an uncertainty (type A and type B) of ± 3% was calculated. As seen in Table III and relevant for the VMPPT algorithm, each row of PV cells have a different value for V_{oc}.

As a result of these differences in V_{oc}, each row of PV cells would require an individual MPPT. In the following example, we illustrate the impact on the obtained output power (P_{out}) if V_{oc} is measured from only one row of PV cells and then used to control PV cells in other rows. For example, V_{oc} is obtained from row number (1) and then used to set the operating voltage (V_{op}) for the PV cells in row number (9) and vice versa. While λ, the V_{oc} and I_{sc} were obtained in experiments, the output power of the MPPT algorithm was calculated with the help of a PV simulation model. At first, we calculate a suitable value for the factor M_V:

at STC (λ = 1,000 W/m^2):

$$M_V = \frac{V_{mpp}}{V_{oc}} = \frac{0.515\,V}{0.613\,V} = 0.84$$

Then, this value for M_V is used to approximate the voltage in the MPP (V_{mpp}) and the available output power (P_{out}).

row (1):

$$\begin{aligned} P_{out} &= V_{op} \times I_{out} = \\ &= M_V \times V_{oc} \times I_{out} = \\ &= 3.114\,W && \text{with } V_{oc} = 0.606 \text{ V} \\ &= 3.075\,W && \text{with } V_{oc} = 0.591 \text{ V} \end{aligned}$$

row (9):

$$\begin{aligned} P_{out} &= V_{op} \times I_{out} = \\ &= M_V \times V_{oc} \times I_{out} = \\ &= 1.859\,W && \text{with } V_{oc} = 0.591 \text{ V} \\ &= 1.860\,W && \text{with } V_{oc} = 0.606 \text{ V} \end{aligned}$$

At the given ambient conditions, P_{mpp} = 3.122 W for PV cells in row number (1) and P_{mpp} = 1.861 W for PV cells in row number (9). Using V_{oc} = 0.606 V results in an MPPT efficiency (η_{mppt}) of 99.7%. However, using V_{oc} = 0.591 V to approximate V_{mpp} results in an MPPT efficiency of 98.5%. In the other case, P_{out} increases slightly if the value for V_{oc} is used from row number (1) for setting the operating voltage of row number (9). This is the situation because the factor M_V is an approximation and not an actual measurement of the position of the MPP. However, generally speaking, the value of M_V should increase if λ increases.

D. Impacts on the Short-Circuit Current (I_{sc})

Similarly to the VMPPT algorithm, the performance of the CMPPT algorithm was evaluated. At first, we calculate a suitable value for the factor M_I:

TABLE II
LONGITUDIAL ANGLES OF PV CELLS ON THE ROOF OF THE TOYOTA PRIUS

	row (1)	row (2)	row (3)	row (4)	row (5)	row (6)	row (7)	row (8)	row (9)
angle	15 °	12 °	9 °	3 °	2 °	0 °	– 3 °	– 7 °	– 9 °

TABLE III
OBTAINED OPEN-CIRCUIT VOLTAGE OF PV CELLS (V_{oc}) AT DIFFERENT SOLAR RADIATION LEVELS

	solar radiation level in row number (6), β = 0 °						
	λ = 570 W/m^2	λ = 590 W/m^2	λ = 620 W/m^2	λ = 630 W/m^2	λ = 640 W/m^2	λ = 650 W/m^2	λ = 660 W/m^2
row (1)	V_{oc} = 0.606 V	V_{oc} = 0.606 V	V_{oc} = 0.608 V	V_{oc} = 0.608 V	V_{oc} = 0.608 V	V_{oc} = 0.608 V	V_{oc} = 0.609 V
row (2)	V_{oc} = 0.603 V	V_{oc} = 0.605 V	V_{oc} = 0.606 V	V_{oc} = 0.606 V	V_{oc} = 0.606 V	V_{oc} = 0.607 V	V_{oc} = 0.607 V
row (3)	V_{oc} = 0.603 V	V_{oc} = 0.604 V	V_{oc} = 0.606 V	V_{oc} = 0.605 V	V_{oc} = 0.605 V	V_{oc} = 0.606 V	V_{oc} = 0.607 V
row (4)	V_{oc} = 0.600 V	V_{oc} = 0.601 V	V_{oc} = 0.603 V	V_{oc} = 0.603 V	V_{oc} = 0.603 V	V_{oc} = 0.603 V	V_{oc} = 0.604 V
row (5)	V_{oc} = 0.599 V	V_{oc} = 0.601 V	V_{oc} = 0.602 V	V_{oc} = 0.602 V	V_{oc} = 0.603 V	V_{oc} = 0.603 V	V_{oc} = 0.604 V
row (6)	V_{oc} = 0.598 V	V_{oc} = 0.599 V	V_{oc} = 0.601 V	V_{oc} = 0.601 V	V_{oc} = 0.602 V	V_{oc} = 0.602 V	V_{oc} = 0.603 V
row (7)	V_{oc} = 0.595 V	V_{oc} = 0.596 V	V_{oc} = 0.598 V	V_{oc} = 0.598 V	V_{oc} = 0.599 V	V_{oc} = 0.600 V	V_{oc} = 0.601 V
row (8)	V_{oc} = 0.592 V	V_{oc} = 0.594 V	V_{oc} = 0.596 V	V_{oc} = 0.597 V	V_{oc} = 0.597 V	V_{oc} = 0.597 V	V_{oc} = 0.598 V
row (9)	V_{oc} = 0.591 V	V_{oc} = 0.592 V	V_{oc} = 0.593 V	V_{oc} = 0.594 V	V_{oc} = 0.595 V	V_{oc} = 0.595 V	V_{oc} = 0.597 V

TABLE IV
OBTAINED SHORT-CIRCUIT CURRENT OF PV CELLS (I_{sc}) AT DIFFERENT SOLAR RADIATION LEVELS

	solar radiation level in row number (6), β = 0 °						
	λ = 570 W/m^2	λ = 590 W/m^2	λ = 620 W/m^2	λ = 630 W/m^2	λ = 640 W/m^2	λ = 650 W/m^2	λ = 660 W/m^2
row (1)	I_{sc} = 6.393 A	I_{sc} = 6.570 A	I_{sc} = 6.976 A	I_{sc} = 6.923 A	I_{sc} = 6.861 A	I_{sc} = 6.985 A	I_{sc} = 7.073 A
row (2)	I_{sc} = 5.960 A	I_{sc} = 6.216 A	I_{sc} = 6.517 A	I_{sc} = 6.508 A	I_{sc} = 6.561 A	I_{sc} = 6.702 A	I_{sc} = 6.764 A
row (3)	I_{sc} = 5.846 A	I_{sc} = 5.987 A	I_{sc} = 6.402 A	I_{sc} = 6.393 A	I_{sc} = 6.340 A	I_{sc} = 6.481 A	I_{sc} = 6.649 A
row (4)	I_{sc} = 5.404 A	I_{sc} = 5.492 A	I_{sc} = 5.872 A	I_{sc} = 5.872 A	I_{sc} = 5.898 A	I_{sc} = 6.013 A	I_{sc} = 6.119 A
row (5)	I_{sc} = 5.227 A	I_{sc} = 5.466 A	I_{sc} = 5.757 A	I_{sc} = 5.793 A	I_{sc} = 5.872 A	I_{sc} = 5.925 A	I_{sc} = 6.084 A
row (6)	I_{sc} = 5.033 A	I_{sc} = 5.210 A	I_{sc} = 5.475 A	I_{sc} = 5.563 A	I_{sc} = 5.651 A	I_{sc} = 5.740 A	I_{sc} = 5.828 A
row (7)	I_{sc} = 4.477 A	I_{sc} = 4.698 A	I_{sc} = 5.033 A	I_{sc} = 5.060 A	I_{sc} = 5.148 A	I_{sc} = 5.395 A	I_{sc} = 5.431 A
row (8)	I_{sc} = 4.124 A	I_{sc} = 4.362 A	I_{sc} = 4.759 A	I_{sc} = 4.777 A	I_{sc} = 4.901 A	I_{sc} = 4.883 A	I_{sc} = 4.989 A
row (9)	I_{sc} = 3.929 A	I_{sc} = 4.088 A	I_{sc} = 4.256 A	I_{sc} = 4.406 A	I_{sc} = 4.565 A	I_{sc} = 4.556 A	I_{sc} = 4.786 A

at STC (λ = 1,000 W/m^2):

$$M_I = \frac{I_{mpp}}{I_{sc}} = \frac{8.039\,V}{8.602\,V} = 0.93$$

Then, this value for M_I is used to approximate the current in the MPP (I_{mpp}) and the available output power (P_{out}).

row (1):

$$\begin{aligned} P_{out} &= I_{op} \times V_{out} = \\ &= M_I \times I_{sc} \times V_{out} = \\ &= 3.115\,W \quad \text{with } I_{sc} = 6.393 \text{ A} \\ &= 2.119\,W \quad \text{with } I_{sc} = 3.929 \text{ A} \end{aligned}$$

row (9):

$$\begin{aligned} P_{out} &= I_{op} \times V_{out} = \\ &= M_I \times I_{sc} \times V_{out} = \\ &= 1.860\,W \quad \text{with } I_{sc} = 3.929 \text{ A} \\ &= 0\,W \quad \text{with } I_{sc} = 6.393 \text{ A} \end{aligned}$$

With the help of the suitable values for I_{sc}, η_{mppt} = 99.8% in row number (1) and η_{mppt} = 99.9% in row number (9). However, the efficiency drops to η_{mppt} = 67.9% if the value for I_{sc} is used from row number (9) for the control of the PV cells in row number (1). Furthermore, as the available current from the PV cells in row number (9) is significantly lower than the current in row number (1), the PV cells in row number (9) cannot be controlled with the current from row number (1). Even I_{sc} of row number (9) is lower than $M_I \times I_{sc}$ obtained from row number (1).

In the CMPPT algorithm, one value for I_{sc} can partly work for PV cells in rows which are facing the sun, but does not work for PV cells which are facing away from the sun. In other words, the different longitudinal angles of PV cells are more critical for the CMPPT algorithm than for the VMPPT algorithm. As the short-circuit current (I_{sc}) is directly proportional to the solar radiation level (λ), variations in I_{sc} are much stronger for PV cells with different longitudinal angles than variations in the open-circuit voltage (V_{oc}). As a result, η_{mppt} of the CMPPT algorithm is reduced significantly

if the same value for I_{sc} is used for PV cells with different longitudinal angles.

E. Measurement Probe and Measurement Setup

The short-circuit current (I_{sc}) of a PV cell is directly proportional to the solar radiation level (λ). This linear relationship was utilised to measure λ and, thus, the rate of change of the solar radiation level (r_λ) with the help of a small PV cell (size: 5 x 5 cm), as illustrated in Fig. 4 and as obtained as follows

$$\lambda \propto I_{out} = I_{sense} = \frac{V_{sense}}{R_{sense}} \quad \text{whereas} \quad V_{sense,max} \ll V_{oc} \tag{4}$$

where V_{sense} is the voltage, which was measured by the National Instruments (NI) USB-6009 data acquisition (DAQ) module; and R_{sense} is the resistor for the current measurement.

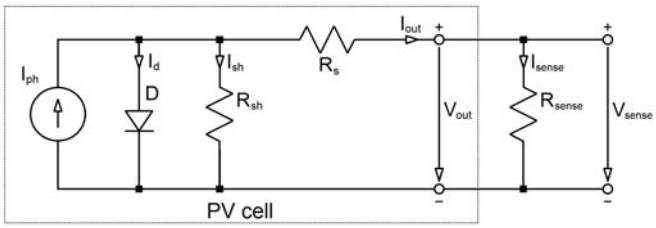

Fig. 4. Equivalent circuit of a PV cell and sense resistor (R_{sense})

Fig. 5 illustrates I-V curves of the PV cell used in the measurement probe under various solar radiation levels and at a PV cell temperature (T_c) of 25 °C. For the measurements under outdoor environmental conditions, the estimated uncertainty was 0.2 °C. The size of R_{sense} was vital and was selected in order to stay in the linear range of the used PV cell in the measurement probe. Hence, we chose R_{sense} as 53.6 Ω, as illustrated in Fig. 5. We mounted measurement probes on the vehicle's roof in order to collect data on the rate of change of the solar radiation level (r_λ) during driving conditions. The measurement probe can also be used for other types of vehicles.

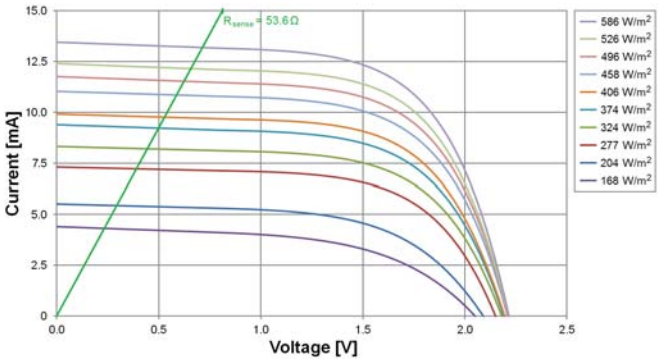

Fig. 5. *I-V* curves of the PV cell used as measurement probe (T_c= 25 °C)

F. Solar Radiation Level during Driving Conditions

In order to understand the available output power of PV cells on top of BEVs and HEVs in more detail, we studied the range of irradiation changes in dynamic conditions. More precisely, we investigated how changes in the solar radiation level are influencing the performance of MPPT algorithms when a vehicle with a PV installation is in driving conditions. Therefore, we determined the slopes of the measured solar radiation changes. For our analysis, we used two data sets which we obtained under the same circumstances as in previous research [11]. In these data sets, measurements were taken on the available solar radiation level while driving in a street surrounded by a trees, buildings and parking lots.

The measurement data helps us to illustrate how rapidly the solar radiation level changes on top of the roof of vehicles when they are driving in urban areas. In both measurements, we calculated the time difference in milliseconds (Δt) which corresponds to the 6,000 adjacent samples of the original data set. We used linear fitting to calculate the rate of change (r_λ) over a set of six data points. This procedure was repeated over the whole measurement data. Figs. 6 and 7 show the obtained results of the two representative data sets on the rate of change of the solar radiation level (r_λ).

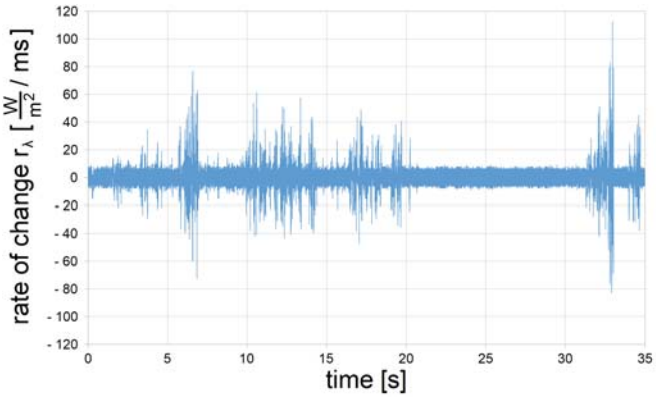

Fig. 6. Rate of change of the solar radiation level (r_λ) for data set 1

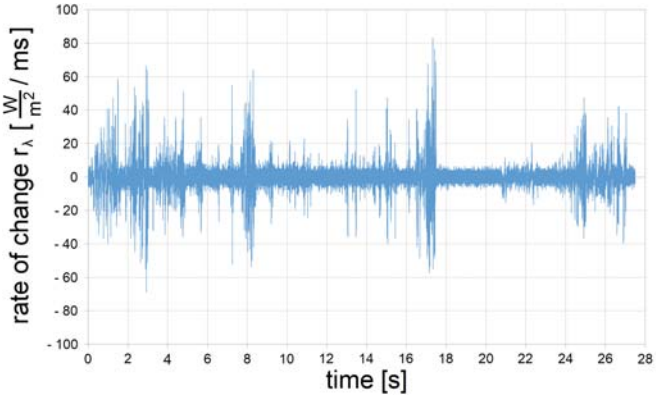

Fig. 7. Rate of change of the solar radiation level (r_λ) for data set 2

As shown in Figs. 6 and 7, r_λ varies between – 80 to 80 $\frac{W}{m^2}/s$. The fastest rate changes are mostly caused by large objects such as trees and buildings creating shadows with

sharp edges. However, it is worth noting that even in the case large shadowing objects are not in the proximity of the PV installation of top of the vehicle, approximately $\pm$ 10 $\frac{W}{m^2}/s$ fluctuation are observed; as for example seen in Fig. 6 between t = 21 ms to 32 ms). This is assumed to be caused by diffuse reflectance and other indirect irradiations to PV cells.

Fig. 8 shows the distribution of r_λ for data set 2. While for stationary PV installations changes of the solar radiation level are taking place in seconds, in the case of moving PV installations, changes in the solar radiation level occur in milliseconds [11]. Generally speaking, variations in the solar radiation level have a direct impact on the available output power of a PV cell and the MPPT algorithm. A variation of 10 W/m^2 causes a change in the available output power (P_{sc}) of 1.32%.

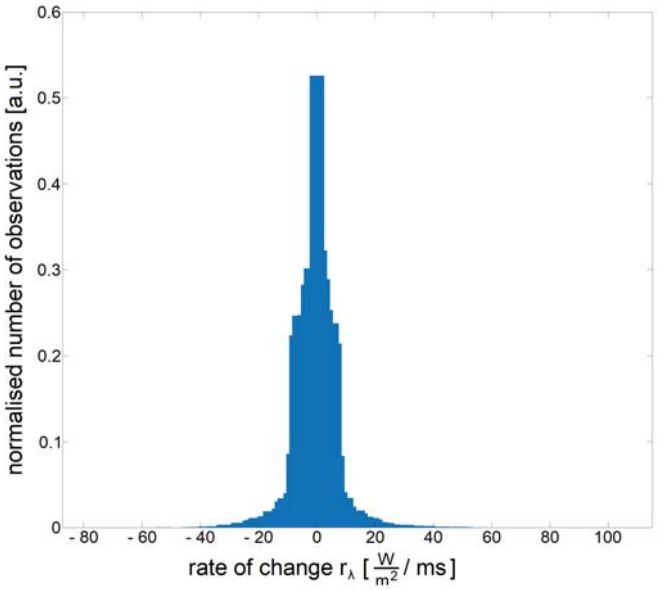

Fig. 8. Distribution of r_λ for data set 2

As seen in Figs. 6 and 7, within a few milliseconds, the solar radiation level can change drastically. Commonly, MPPT algorithms sense the voltage and/or current in a time window of 5 to 15 seconds. Hence, the information of the voltage and/or current can be out of date, shortly after the information was obtained as the solar radiation level has already changed. These circumstances will have an impact on the efficiency of the MPPT algorithm and the obtained output power of PV cells.

V. Conclusion

Due to the curved shape of the roof of BEVs and HEVs, each PV cell will face the sun under a different longitudinal angle. As a result, each PV cell receives a different solar radiation level. On the example of the Toyota Prius, we presented experimental data indicating the large variations in the obtained open-circuit voltage (V_{oc}) and short-circuit current (I_{sc}) of PV cells with different longitudinal angles. We demonstrated that these variations have an impact on the available output power and MPPT algorithms.

When PV cells are connected in series, the weakest PV cell of the interconnection will determine the available output power. As the available solar radiation level is different for each PV cell, it can be advisable to control each PV cell individually with a MPP tracker. Due to the limited area for deploying PV cells on top of BEVs and HEVs, one of the main objectives lies in the optimisation of the efficiency. Fast slopes of the solar radiation level during driving conditions will make this optimisation more complex. Hence, it is expected that the efficiency of MPPT algorithms is lower for moving PV installations than for stationary PV installations.

Acknowledgment

We wish to thank Infotech Oulu for financially supporting this research. Prof. Tapio Fabritius was partially funded by the Academy of Finland 6Genesis (6G) project. We appreciate Harald Gall, Klaus Eberhart, Hannes Illko, Suzy McAnsh and Maija Schuss for their help and comments on this research work.

References

[1] D.P. van Vuuren, N. Nakicenovic, K. Riahi, A. Brew-Hammond, D. Kammen, V. Modi, and K. Smith, "An energy vision: The transformation towards sustainability - interconnected challenges and solutions", *Current Opinion in Environmental Sustainability*, vol. 4, issue: 1, pp. 18-34, 2012.

[2] S. Mekhilef, R. Saidur, and A. Safari, "A review on solar energy use in industries", *Renewable and Sustainable Energy Reviews*, vol. 15, issue: 4, pp. 1777-1790, 2011.

[3] C. Schuss, H. Gall, K. Eberhart, H. Illko, and B. Eichberger, "Alignment and Interconnection of Photovoltaics on Electric and Hybrid Electric Vehicles", *Proceedings of the IEEE International Instrumentation and Measurement Technology Conference (I2MTC)*, pp. 524-527, 2014.

[4] K. Araki, L. Ji, G. Kelly, and M. Yamaguchi, "To Do List for Research and Development and International Standardization to Achieve the Goal of Running a Majority of Electric Vehicles on Solar Energy", *Coatings*, vol. 8, issue: 7, pp. 251, 2018.

[5] T. Masuda, K. Araki, K. Okumura, S. Urabe, Y. Kudo, K. Kimura, T. Nakado, A. Sato, and M. Yamaguchi, "Static concentrator photovoltaics for automotive applications", *Solar Energy*, vol. 146, pp. 523-531, 2017.

[6] K. Araki, C. Algora, G. Siefer, K. Nishioka, R. Leutz, S. Carter, S. Wang, S. Askins, L. Ji, and G. Kelly, "Standardization of the CPV and car-roof PV technology in 2018 - Where are we going to go?", *AIP Conference Proceedings*, vol. 2012, no. 1, p. 070001, 2018.

[7] G.C. Mouli, P. Bauer, and M. Zeman, "System design for a solar powered electric vehicle charging station for workplaces", *Applied Energy*, vol. 168, pp. 434-443, 2016.

[8] G. Leen, and D. Heffernan, "Expanding automotive systems", *Computer*, vol. 35, issue: 1, pp. 88-93, 2002.

[9] E. Karden, S. Ploumen, B. Fricke, T. Miller, and K. Snyder, "Energy storage devices for future hybrid electric vehicles", *Journal of Power Sources*, vol. 168, issue: 1, pp. 2-11, 2007.

[10] M.A. Hussin, A.N. Abdalla, R. Ishak, R. Abdullah, and Z.M. Ali, "Study on Improving Electric Vehicle drive range using Solar Energy", *International Conference on Electrical, Control and Computer Engineering (InECCE)*, pp. 373-376, June 2011.

[11] C. Schuss, B. Eichberger, and T. Rahkonen, "Impact of Solar Radiation on the Output Power of Moving Photovoltaic (PV) Installations", *Proceedings of the IEEE International Instrumentation and Measurement Technology Conference (I2MTC)*, pp. 1297-1302, 2018.

[12] Blue Chip Energy GmbH. 2010_02_01_BCE_QM_Kde_SAP-Zelle_V3 (in German) Available online: www.bluechip-energy.at (accessed on 6 August 2010).

[13] T. Esram, and P.L. Chapman, "Comparison of Photovoltaic Array Maximum Power Point Tracking Techniques", *IEEE Transactions on Energy Conversion*, vol. 22, issue: 2, pp. 439-449, 2007.